



HAL
open science

Surface properties of hydrogenated nanodiamonds: a chemical investigation

Hugues Girard, Tristan Petit, S. Perruchas, T. Gacoin, Céline Gesset,
Jean-Charles Arnault, Philippe Bergonzo

► To cite this version:

Hugues Girard, Tristan Petit, S. Perruchas, T. Gacoin, Céline Gesset, et al.. Surface properties of hydrogenated nanodiamonds: a chemical investigation. *Physical Chemistry Chemical Physics*, 2011, 13 (24), pp.11517-11523. 10.1039/c1cp20424f. cea-01807359

HAL Id: cea-01807359

<https://cea.hal.science/cea-01807359>

Submitted on 25 Jul 2023

HAL is a multi-disciplinary open access archive for the deposit and dissemination of scientific research documents, whether they are published or not. The documents may come from teaching and research institutions in France or abroad, or from public or private research centers.

L'archive ouverte pluridisciplinaire **HAL**, est destinée au dépôt et à la diffusion de documents scientifiques de niveau recherche, publiés ou non, émanant des établissements d'enseignement et de recherche français ou étrangers, des laboratoires publics ou privés.

1 Cite this: DOI: 10.1039/c1cp20424f

5 www.rsc.org/pccp

Q1 Surface properties of hydrogenated nanodiamonds: a chemical investigation†10 H. A. Girard,^{*a} T. Petit,^a S. Perruchas,^b T. Gacoin,^b C. Gesset,^a J. C. Arnault^a
and P. Bergonzo^a

Received 17th February 2011, Accepted 8th April 2011

15 DOI: 10.1039/c1cp20424f

Hydrogen terminations (C–H) confer to diamond layers specific surface properties such as a negative electron affinity and a superficial conductive layer, opening the way to specific functionalization routes. For example, efficient covalent bonding of diazonium salts or of alkene moieties can be performed on hydrogenated diamond thin films, owing to electronic exchanges at the interface. Here, we report on the chemical reactivity of fully hydrogenated High Pressure High Temperature (HPHT) nanodiamonds (H-NDs) towards such grafting, with respect to the reactivity of as-received NDs. Chemical characterizations such as FTIR, XPS analysis and Zeta potential measurements reveal a clear selectivity of such couplings on H-NDs, suggesting that C–H related surface properties remain dominant even on particles at the nanoscale. These results on hydrogenated NDs open up the route to a broad range of new functionalizations for innovative NDs applications development.

30 Introduction

Diamond nanoparticles or nanodiamonds (NDs) containing nitrogen-vacancy (N-V) coloured centres hold great promises for biomedical applications.¹ They combine some of the outstanding properties of bulk diamond, such as its chemical resilience and its carbon surface chemistry, further to the benefits of hosting a photoluminescent centre emitting in the far-red with a remarkable photostability.² While their mass production is now well controlled^{3–5} and their low cytotoxicity reported,^{6–8} NDs appear as very promising biolabels for both diagnostic and therapeutic applications.⁹

The use of NDs to label biomolecules or to deliver bioactive molecules implies however that specific chemical functionality can be granted to the bare NDs. Their stability in biological media, their role to target or to release drug, go through a suitable surface functionalization of the particles with, for instance, PEG chains, proteins or ionic moieties.^{9–13} However, after post-synthesis purification treatments and irradiation/annealing to create N-V centres, ND surface chemistry remains highly inhomogeneous. Amorphous carbon, graphite shells and various oxidized terminations, from ether to acid groups, are amenable to cover the diamond particles.¹⁴ Direct functionalization on such NDs leads to an inhomogeneous

and uncontrolled surface chemistry. Intense research efforts are thus dedicated to the surface homogenization of the particles, since the functionalization efficiency strongly depends on the initial NDs surface terminations. Chemical treatments can be used to either promote the formation of COOH¹¹ or C–OH groups,¹⁵ known as starting points towards amidation, esterification or silanization grafting routes. Such wet chemistry treatments are efficient but may lead to a contamination of the NDs by chemical reagents or reaction sub-products, and thus require numerous washing steps, often considered as time and effort consuming. Annealings under controlled atmosphere such as fluorine, argon, oxygen, or *in vacuo* are other ways to homogenize the ND surface chemistry and to create new surface terminations.^{16,17} However, high temperatures can easily lead to the degradation of the diamond surface and the formation of amorphous and sp² carbon on NDs.¹⁸

In this context, we have developed an alternative route, based on hydrogen plasma treatment in a microwave (MW) cavity.¹⁹ Atomic hydrogen created under MW chemical vapour deposition (MWCVD) conditions is able to reduce oxygenated terminations into hydrogenated ones with high efficiency and, at the same time, to prevent from the formation of sp² and amorphous carbon species. This dry treatment leads to fully hydrogenated NDs (H-NDs) ready to be used, without any further chemical purification steps. This leads to large quantities of H-NDs with almost full hydrogenated surface termination to be produced, as confirmed by various characterization techniques (FTIR, XPS, Raman), all revealing the spectroscopic signatures of hydrogenated diamond layers.

55 ^aCEA, LIST, Diamond Sensors Laboratory, 91191 Gif sur Yvette, France. E-mail: hugues.girard@cea.fr^bCNRS-Ecole Polytechnique, Laboratoire de Physique de la Matière Condensée, 91128 Palaiseau, France

† Electronic supplementary information (ESI) available. See DOI: 10.1039/c1cp20424f

1 Herein, we report investigations addressing the study of the
chemical reactivity of these H-NDs exposed to three different
surface modifications: selective oxidation under UV exposure,
as well as two grafting routes with alkenes and diazonium
5 moieties. These reactions are common on hydrogenated
diamond films towards efficient biological functionalizations
(DNA, proteins grafting)^{20–22} so their use on NDs may also
lead to promising developments. However, the chemical
mechanisms involved in these grafting routes require specific
10 surface properties, involving charge transfer, which is
only provided to the diamond surface by C–H hydrogen
terminations.²³ Therefore, this article aims at evaluating if this
specific reactivity also exists on H-NDs by studying their
reactivity towards those three “standard” chemical reactions.
15 In this way, experiments performed on as-received NDs and
H-NDs will be compared.

Experimental

Materials and chemicals

20 High Pressure High Temperature (HPHT) NDs (mean
diameter: 50 nm) were purchased from Van Moppes (Syndia®
SYP 0-0.05). Acetonitrile (Riedel-De Haën), pentane (VWR),
25 4-nitrophenyldiazonium tetrafluoroborate (Aldrich) and
undecylenic acid (Aldrich) were used as received.

Hydrogenation

30 The experimental procedure used for the hydrogenation has
been previously reported in details.¹⁹ Briefly, 100 mg of NDs
were deposited in a quartz cartridge and introduced in a sealed
quartz tube. Hydrogen was injected at pressures up to 10 mbar
and plasma was generated in the quartz tube with a microwave
35 power of 300 W. Homogenization of the NDs in the hydrogen
plasma was optimized by a rotation of the quartz tube. NDs
were exposed to hydrogen plasma for 20 minutes leading to
H-NDs.

UV hydroxylation

40 After hydrogenation, H-NDs are kept in their quartz cartridge
and exposed to a H₂O vapour saturated atmosphere. The
cartridge is then illuminated using a 254 nm UV lamp for
6 hours. NDs are mixed by rotating the quartz pipe.

UV alkene grafting

45 20 mg of H-NDs were reacted with 5 mL of pure degassed
undecylenic acid under 254 nm UV lamp for 12 h. After
reaction, NDs were washed by 7 successive centrifugation

and redispersion cycles in acetic acid, acetone and water prior
to the drying of the solid residue under primary vacuum.

Diazonium grafting

5 20 mg of H-NDs were reacted with 60 mg (2.5×10^{-4} mol) of
4-nitrophenyldiazonium tetrafluoroborate in 25 mL of
acetonitrile for 12 h under nitrogen with vigorous stirring.
After reaction, NDs were washed by 5 successive centrifuga-
tion and redispersion cycles in acetonitrile and then the solid
10 residue was dried under primary vacuum.

Characterizations

XPS analyses were performed using an Omicron XPS spectro-
meter equipped with an Al K α monochromatized anode
($h\nu = 1486.6$ eV). The binding energy scale was calibrated
15 *versus* the Au 4f_{7/2} peak located at 84.0 eV.²⁴ Curve fitting was
performed to extract the components in the C1s spectra, using
a fixed Gaussian/Lorentzian ratio of 30%. Peak areas were
determined following the Shirley’s inelastic background
20 subtraction method.²⁵ Atomic ratios were calculated from
the integrated intensities of core levels after photoionization
cross-section corrections.²⁶

FT-IR spectra were measured in a transmission mode using
a Thermo Nicolet 8700 spectrometer. KBr pellets were
25 prepared with as-received NDs, H-NDs (immediately after
hydrogenation) and functionalized NDs. Measurements of
H-NDs and hydroxylated NDs were performed in a home-
made IR vacuum cell connected to a primary vacuum system
(10^{-3} mTorr) and equipped with KBr windows and a heater
30 (400 K). For as-received and reacted NDs, IR measurements
were performed under nitrogen flow.

Zeta potential (ZP) measurements were recorded in solution
at controlled pH on a Malvern ZetaSizer Nano. All experi-
ments were performed with the manufacturer calibration
35 procedures.

Results

The first reaction conducted on H-NDs was UV hydroxylation.
40 Immediately after hydrogen plasma exposure of HPHT
NDs, the quartz pipe was filled up with air and water vapours
and then exposed to UV irradiation for 6 hours (Fig. 1a).
FTIR spectroscopy of the NDs was used to investigate the
chemical modifications induced by this UV treatment. To
45 overcome peaks related to adsorbed water on the spectra,²⁷
treated samples (hydrogenated and hydroxylated) were dried
in an *in situ* IR reactor cell for one night prior to the
measurement as well as during acquisition.²⁸ FTIR spectra
are reported in Fig. 2. As-received and H-NDs spectra are also
50

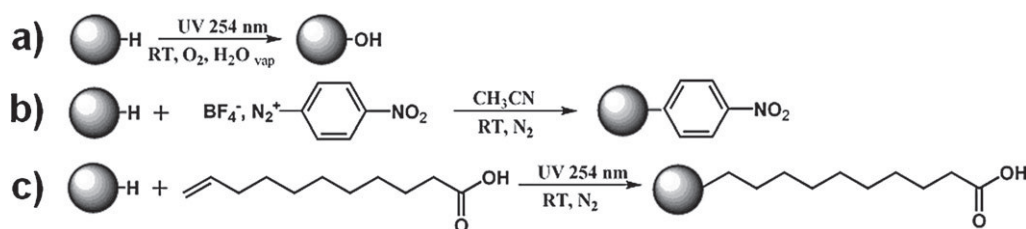


Fig. 1 Schemes of the reactions conducted to functionalize H-NDs.

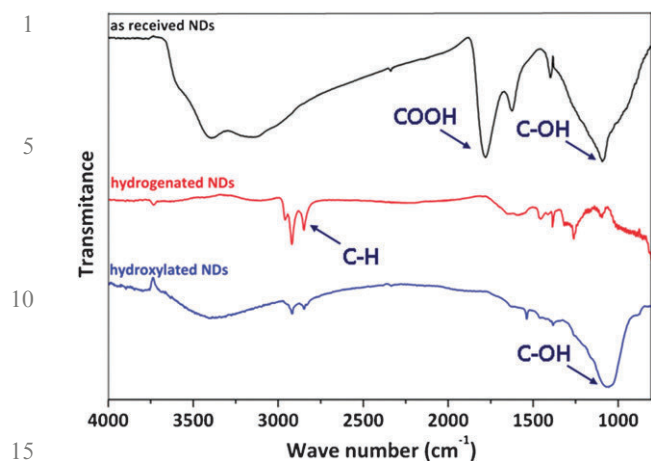


Fig. 2 FTIR spectra of as-received, hydrogenated and hydroxylated NDs.

20 reported for comparison. Hydrogenation is mainly evidenced by the loss of the IR bands at 3300 cm^{-1} , 1770 cm^{-1} and 1050 cm^{-1} , relative to O-H, C=O (in COOH groups) and C-OH terminations, respectively, with the exaltation of the C-H stretching bands.²⁹ After UV treatment, a re-oxidation of the surface occurs, revealed by the re-appearance of C-OH and OH relative bands at 1050 and 3300 cm^{-1} , respectively. Drying treatment prior and during the IR acquisition ensures that these signals are not related to H₂O adsorption. It should be noted that this oxidation method does not lead to the formation of acid groups at the surface, since no acid-related bands (between 1700 and 1800 cm^{-1}) are observed.

XPS analyses were carried out on the hydroxylated NDs. C1s core level spectra of as received, hydrogenated and hydroxylated NDs are reported in Fig. 3a. As previously described,¹⁹ the hydrogenation treatment induces a shift towards lower binding energies, to values close to those probed on hydrogenated undoped layers³⁰ and a decrease of the C1s FWHM (from 2 to 1.4 eV), which is attributed to the loss of the carbon-oxygen related components and the formation of hydrogenated terminations. After hydroxylation, a broadening of the C1s peak occurs. To gain better insights to these modifications, the deconvolution of the hydrogenated and hydroxylated C1s core level spectra was performed (Fig. 3b). Hydrogenated NDs exhibit two main contributions, at 284.8 and 285.5 eV, attributed to C-C sp³ and CH_x(x ≥ 2) bonds respectively.³¹ At higher binding energies (286.7 eV), a very weak contribution can be assigned to oxygenated terminations.

This contribution is in agreement with the 3 at.% of oxygen measured at the sample surface, mostly due to spontaneous reoxidation of the hydrogenated particles during the transfer into the UHV chamber. After hydroxylation, the two main contributions, at 284.8 and 285.5 eV, attributed to C-C sp³ and CH_x(x ≥ 2) bonds, respectively, are still observed, but a new component located at 286.1 eV arises on the C1s spectrum, for 13% of the C1s total area. As reported in the literature, peaks located at this binding energy range are associated with carbon-oxygen single bonded functionalities, such as ether or hydroxyl groups. In a detailed study on diamond oxygenated terminations,³² authors have shown that

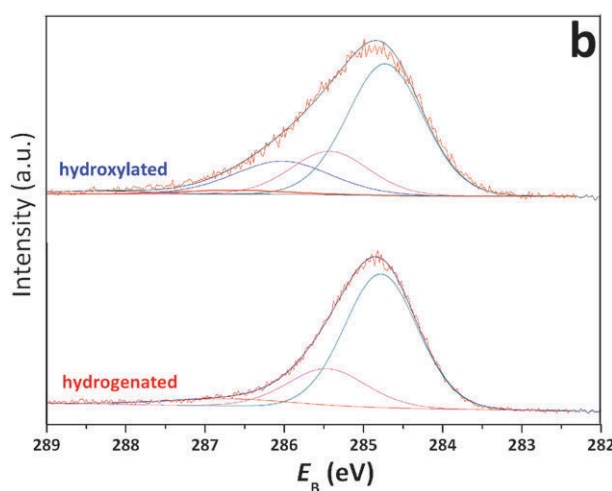
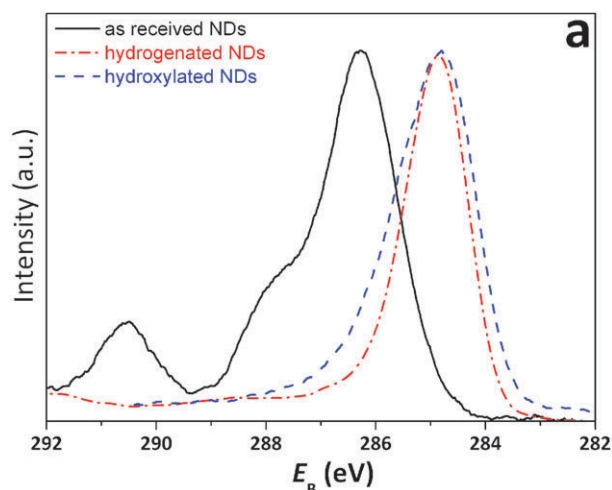


Fig. 3 (a) XPS C1s core levels of as received, hydrogenated and hydroxylated NDs and (b) C1s fits of hydrogenated and hydroxylated NDs.

the components located at +1.2 eV and 1.9 eV from the C-Csp³ peak are, respectively, related to C-OH and C-O-C groups. Here, considering the energy shift (+1.3 eV) and the FTIR data, this new component can be mainly attributed to hydroxyl groups.^{33,34} It should be noted that a very weak component located at higher binding energies (286.9 eV) is still present, and is likely to be due to ether bridges. These results are in agreement with the concomitant oxygen increase, from below 3 to 11 at.% after the hydroxylation treatment. From these results, a surface density of the hydroxyl groups created on the NDs can be estimated at values close to 1 function nm⁻². However, considering the high roughness of the sample induced by the sample preparation (drop casting), this result has to be considered only as a rough estimation and be handled with precaution.

Finally, Zeta potentials at neutral pH were measured on as received and hydroxylated NDs dispersed in water. An inversion of the Zeta potential occurs with values of -45 mV for as received NDs and +30 mV for the hydroxylated ones. This E_{ZETA} switching will be further discussed below.

The second chemical modification performed on H-NDs is also a photochemically induced process. Immediately after

1 hydrogenation, NDs were reacted with pure undecylenic acid, under 254 nm UV irradiation (Fig. 1b). This alkene was chosen for its long alkyl chain and its acid group, both functionalities easily identifiable by FTIR analysis with characteristic structures at 2800 cm^{-1} and 1700 cm^{-1} respectively (Fig. 4a). Furthermore, the vinyl function is evidenced by a peak located around 900 cm^{-1} . For comparison, the same reaction was also conducted on as-received NDs.

Fig. 4a shows the FTIR spectra of H-NDs after reaction with undecylenic acid under UV exposure. It appears clearly that both characteristics of the undecylenic acid structures, at 1700 cm^{-1} and 2800 cm^{-1} , are present on the spectrum after reaction with noticeable intensities. Furthermore, the band related to the vinyl function visible at 900 cm^{-1} on the undecylenic acid spectrum is missing on the reacted H-NDs, confirming the grafting of the moiety by the formation of a stable C-C single bond. Furthermore, if the same experiment is performed without UV exposure, the grafting is strongly hindered, as shown by the FTIR spectrum of Fig. 4a.

Fig. 4b shows the FTIR spectra of as-received NDs under similar conditions. Around $1700\text{--}1800\text{ cm}^{-1}$, a modification of the broad band related to the acid groups of the as-received NDs is observed, suggesting the appearance of a new component

which may be related to the undecylenic acid COOH groups. However, at 2800 cm^{-1} , only a very weak structure is visible. Therefore, despite the modification of the $1700\text{--}1800\text{ cm}^{-1}$ range, grafting of the undecylenic acid on as-received NDs appears as strongly inhibited compared to hydrogenated NDs. Indeed, this evolution of the NDs COOH related band could also be attributed to a modification of the pre-existing oxidized termination of the as-received NDs during the grafting procedure. For instance, an effect of the successive centrifugations can be suggested, as a size-dependent C=O stretching frequency has been revealed on NDs.³⁵

Finally, the third chemical reaction carried out on H-NDs is based on an electroless diazonium grafting, already investigated in a previous study.¹⁹ In this reaction, the reduction of the diazonium group will not be supported by electrochemistry, the charge exchange being based on chemical reactions occurring at the interface.³⁶ As-received as well as H-NDs were exposed in same conditions to a nitrobenzene diazonium salt (Fig. 1c). This diazonium salt was chosen for its nitro group, easily identifiable by FTIR through the ONO stretching bands visible at 1344 and 1520 cm^{-1} . FTIR spectra of the diazonium salt precursor and of reacted NDs are reported in Fig. 5a and b. In addition to the ONO bands, the diazonium salt exhibits a characteristic peak at 2270 cm^{-1} related to the diazonium N_2^+ . On reacted as-received NDs (Fig. 5a), no contribution of the ONO stretching bands is noticeable on the FTIR spectrum. On reacted H-NDs (Fig. 5b), the two ONO related bands at 1344 and 1520 cm^{-1} are clearly visible, while no contribution at 2270 cm^{-1} related to the N_2^+ is evidenced. The coupling occurred between the nitrobenzene moiety and the H-NDs, with the reduction of the N_2^+ into N_2 , as expected for an aryldiazonium reaction in these conditions.³⁶ As no reaction occurred with as-received NDs, a spontaneous selective bonding only on H-NDs is revealed. XPS analyses were performed onto reacted samples. Only carbon, nitrogen and oxygen contributions were revealed. C1s core level of reacted NDs is displayed in Fig. 6. The comparison with C1s core level of freshly hydrogenated NDs (Fig. 3b) shows the presence of a new component located at 283.7 eV , *i.e.* at lower binding energies than the C-C sp^3 peak of the diamond core. According to the literature, this peak can be attributed to the C-C sp^2 conjugated bounds of the phenyl groups.³⁷ It should be noted that this component represents 3% of the C1s core level. At higher binding energies, between 285.5 and 288 eV , slight modifications also occur, attributed to the C-N bounds and re-oxidation of the NDs surface. However, in this range, a strong overlap between C-O and C-N components prevents an accurate deconvolution. Finally, N1s core level (inset Fig. 6) shows the characteristic NO_2 component located at 406 eV . A weaker contribution is also visible at 400 eV , which can be attributed to azo groups ($-\text{N}=\text{N}-$).³⁸ Azo linkages during diazonium coupling have already been reported several times in the literature, but their formation mechanism is still under debate. One can suggest an azo coupling reaction between the diazonium cation and an electron-rich aromatic ring.³⁹ The presence of these azo linkages suggests that a growth of nitrophenyl multilayers is not excluded in our case. Calculations on core level areas reveal a nitrogen atomic

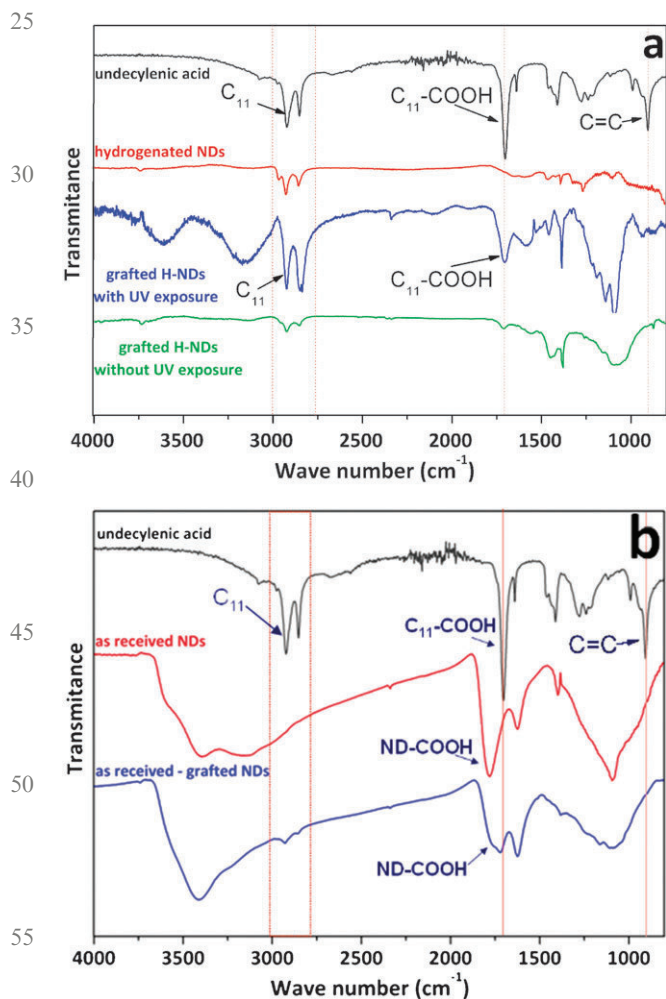


Fig. 4 FTIR spectra of reacted (a) H-NDs and (b) as received NDs with undecylenic acid.

Discussion

Among the several oxidation procedures of diamond, such as electrochemical,⁴⁰ plasma⁴¹ or thermal⁴² methods, UV oxidation of a hydrogenated diamond surface in the presence of O₂ and H₂O appears as the most selective oxidation route.⁴³ Formation of OH radicals introduces a hydroxyl group as surface terminations on diamond to the exclusion of other oxygenated terminations. Other groups have reported on diamond layers successfully hydroxylated by this method, allowing further functionalization by the silanization method.⁴⁴ On H-NDs, this oxidation procedure gives rise to a hydroxylation of the surface, confirmed by the FTIR bands at 1050 and 3300 cm⁻¹ and the new component located at 286.1 eV on the XPS C1s core level (Fig. 3b). Note that after hydroxylation of a hydrogenated diamond thin film, a similar modification of the C1s peak was reported by Szunerits and Boukherroub.³³ Selectivity of this oxidation procedure seems also to be preserved on H-NDs as no carboxyl or carbonyl groups were evidenced by XPS or FTIR. However, inversion of the Zeta potential sign is more difficult to explain. Obviously, the initial negative value at neutral pH is linked to the dissociation of the carboxylic acids present on our as-received NDs (pK_a < 5 if we consider aliphatic carboxylic acids). After hydroxylation treatment, both XPS and FTIR analyses confirmed that no carboxylic acids remain on the surface and only revealed the formation of C–OH groups with an apparently good selectivity. At the same time, a positive Zeta potential was measured. Two distinctive studies in the literature report of a similar phenomenon. Ozawa *et al.* reported on a positive Zeta potential switching after hydroxylation of carboxylated NDs by a reduction with borane. They confirmed the presence of hydroxyl groups on their NDs by FTIR measurements and further silanization coupling.⁴⁵ In this paper, authors do not give any explanation for this charge switching, but their particles were not submitted to a hydrogenation pre-treatment. This last point excludes in our case an effect of remaining C–H terminations on the charge switching. Williams *et al.*⁴⁶ reported on a positive Zeta value switching of NDs after an annealing at 500 °C in hydrogen gas. They showed by FTIR analysis a desorption of carboxylic functionalities and formation of CH, CH₂ and CH₃ groups. They also noticed that a reduced concentration of oxygen-containing groups like ether, alcohol and ketones remained on their particles. In this study, authors refute that protonation of these oxygen-containing groups can occur at neutral pH in water. They suggest an explanation based on Electron-Donor–Acceptor (EDA) complexes which can interact with oxonium ions in water (H₃O⁺). However, such complexes require sp² bonding on the particles, which was not revealed by the XPS analysis performed on our particles. Therefore, at this stage, a link between the positive Zeta potential value and the hydroxylation cannot be strictly established, but further experiments are under progress. Anyway, H-NDs show the same reactivity and selectivity towards the UV oxidation process than hydrogenated diamond layers. These results point out the homogeneity and the quality of the hydrogenated terminations created by MPCVD on the NDs, comparable to hydrogenated diamond layers. Furthermore,

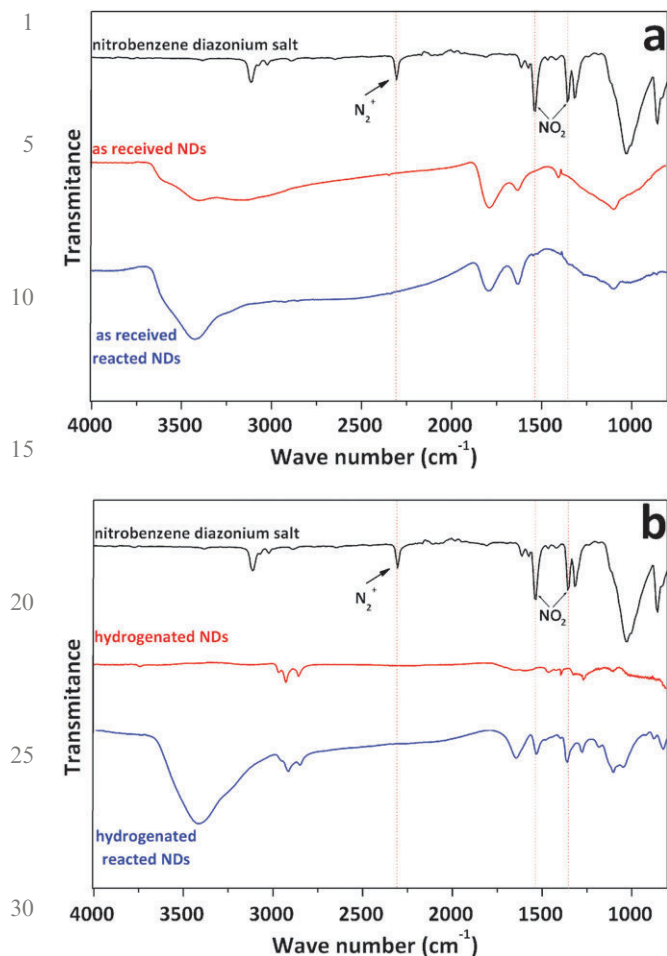


Fig. 5 FTIR spectra of reacted (a) as received and (b) H-NDs with diazonium salt.

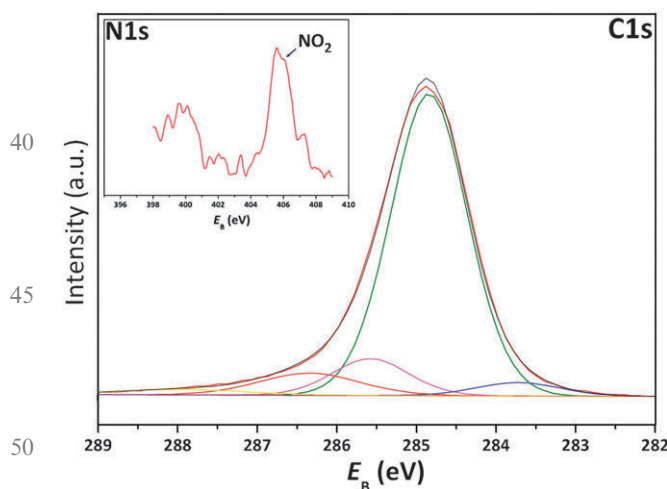


Fig. 6 XPS C1s and N1s (inset) core levels of hydrogenated NDs reacted with nitrobenzene diazonium salt.

concentration of 3.3% after grafting. Considering the approximations previously described, this ratio allows us to estimate a grafting density between 0.5 and 1 function nm⁻², which is in the same range as reported for hydrogenated diamond layers.³⁷

1 this experiment demonstrates that hydroxylation of NDs can
be easily conducted by this selective method, avoiding the risk
of contamination of the NDs with a chemical reduction.

2 The comparison between the reactivity of the hydrogenated
3 and the as-received NDs towards diazonium and alkene
coupling undoubtedly reveals a higher efficiency of these
grafting routes for H-NDs. On diamond layers, numerous
studies report that C–H strongly enhances both chemical
reactions,²³ leading to the formation of covalent C–C bonds
10 between the diamond surface and the grafted moiety. Indeed,
hydrogenated terminations confer to the diamond layers
specific electronic surface properties, such as a superficial
conductive layer⁴⁷ (SCL) and a negative electron affinity^{48,49}
(NEA). The latter is usually highlighted to explain the
15 reactivity of hydrogenated diamond layers towards alkenes,
by the mean of photo-excited electrons allowed to propagate
out of the diamond into the nearby liquid phase, even with
sub-bandgap excitation.⁵⁰ If the mechanisms of this chemical
reaction between the hydrogenated diamond layer and the
20 alkene moiety are still not clearly established, authors agree
that hydrogen terminations are required for this reaction, and
that electron transfer arises from sp³ surfaces and not from
grain boundaries and/or sp² species at the interface.
Oxygenated terminations inhibit the reaction, as the electron
25 affinity of the material turns from negative to positive.⁵¹
Transferred onto H-NDs, the same phenomenon seems to
occur, with the same selectivity of the reaction towards the
nature of the surface terminations. For as-received NDs,
covered with oxygenated terminations (see the FTIR spectrum
30 of Fig. 2), the reaction between the alkene and the ND surface
is inhibited. On the other hand, when hydrogenated, the
reaction clearly leads to a successful functionalization of the
ND surface. Finally, if H-NDs are not submitted to a UV
exposure during the grafting, the reaction is also strongly
35 inhibited. This confirms that the reaction is promoted by
photons. All these results point out a similar behaviour
between hydrogenated diamond layers and nanoparticles,
suggesting a negative electron affinity on 50 nm H-NDs.

4 In the same way, the spontaneous grafting of a diazonium
salt on a diamond surface also arises from specific electronic
properties conferred by C–H terminations.³⁷ The covalent
bonding goes through the creation of a phenyl radical by the
mean of an electron transfer from the diamond surface to the
aryldiazonium salt.³⁷ In this case, the electron transfer is due
45 to the presence of a superficial conductive layer, a p-type layer.
The commonly accepted mechanism, so-called *transfer doping*,⁴⁷
describes a hole accumulation layer due to an electron transfer
from the valence band and a redox couple adsorbed on the
surface when the diamond is exposed to wet atmosphere or
50 immersed in an electrolyte. This phenomenon is only possible
on hydrogenated layers which exhibit a low ionization
potential, matching with the chemical potentials of the adsor-
bates. On oxygenated layers, exhibiting higher ionization
potential, this surface conductivity and the related electron
55 transfer vanishes.⁵¹ As for alkene grafting, a comparison
between diamond layers and nanoparticles reactivity towards
diazonium moieties can now be established. In our experi-
ments, spontaneous grafting of the diazonium moiety only
occurs on H-NDs, with a high grafting density. As-received

NDs, carrying mostly oxygenated terminations, exhibit a very
poor reactivity towards diazonium salt. Examples of successful
diazonium grafting on oxygenated NDs have been reported in
the literature, but always with the help of an external energy
source (sonication or high energy milling process),^{28,52} used to
5 break the C–N bonds and/or to induce damages to the
diamond phase. Graphitization of the NDs can also enhance
this reaction.²⁸ On H-NDs, no graphite could be probed using
Raman or XPS analysis. Therefore, excluding the effect of sp²
species or external energy, the spontaneous coupling onto our
10 H-NDs and its selectivity towards the termination nature
strongly suggests a similar grafting mechanism than for
diamond layers. The presence of a negative electron affinity
and a superficial conductive layer on H-NDs appears as the
most convincing argument to explain this reactivity. 15

Conclusions

In this study, high quality and homogeneous hydrogenated
nanodiamonds were reacted according to standard reactions
20 commonly performed onto hydrogenated diamond layers.
A selective oxidation process involving UV exposure, a photo-
chemical reaction with alkenes and a coupling of diazonium
salts were tested on as-received (oxidized) and hydrogenated
NDs and grafting efficiencies were compared. All the results
25 demonstrate a very similar chemical behaviour with diamond
layers, with the same selectivity towards terminations nature
(hydrogenated or oxygenated). As this selectivity is known to
be associated with specific surface properties on hydrogenated
layers, NEA and SCL, we suggest that similar surface properties
30 arises for the 50 nm HPHT hydrogenated particles.

Acknowledgements

H. A. Girard acknowledges the NADIA project (ANR-PNANO
35 07-045) for a 2008–2010 postdoctoral fellowship.

References

- 1 A. M. Schrand, S. A. C. Hens and O. A. Shenderova, *Crit. Rev. Solid State Mater. Sci.*, 2009, **34**, 18. 40
- 2 S.-J. Yu, M.-W. Kang, H.-C. Chang, K.-M. Chen and Y.-C. Yu, *J. Am. Chem. Soc.*, 2005, **127**, 17604.
- 3 Y.-R. Chang, H.-Y. Lee, K. Chen, C.-C. Chang, D.-S. Tsai, C.-C. Fu, T.-S. Lim, Y.-K. Tzeng, C.-Y. Fang, C.-C. Han, H.-C. Chang and W. Fann, *Nanotechnol.*, 2008, **3**, 284.
- 4 G. Dantelle, A. Slablab, L. Rondin, F. Lainé, F. Carrel, P. Bergonzo, S. Perruchas, T. Gacoin, F. Treussart and J.-F. Roch, *J. Lumin.*, 2010, **130**, 1655. 45
- 5 T.-L. Wee, Y.-W. Mau, C.-Y. Fang, H.-L. Hsu, C.-C. Han and H.-C. Chang, *Diamond Relat. Mater.*, 2009, **18**, 567.
- 6 V. Vijayanthimala, Y.-K. Tzeng, H.-C. Chang and C.-L. Li, *Nanotechnology*, 2009, **20**, 425103.
- 7 Y. Yuan, X. Wang, G. Jia, J.-H. Liu, T. Wang, Y. Gu, S.-T. Yang, S. Zhen, H. Wang and Y. Liu, *Diamond Relat. Mater.*, 2010, **19**, 291. 50
- 8 A. M. Schrand, H. Huang, C. Carlson, J. J. Schlager, E. ÅEsawa, S. M. Hussain and L. Dai, *J. Phys. Chem. B*, 2007, **111**, 2.
- 9 H. Huang, E. Pierstorff, E. Osawa and D. Ho, *Nano Lett.*, 2007, **7**, 3305. 55
- 10 H. J. Huang, E. Pierstorff, E. Osawa and D. Ho, *ACS Nano*, 2008, **2**, 203.
- 11 L.-C. L. Huang and H.-C. Chang, *Langmuir*, 2004, **20**, 5879.
- 12 V. Grichko, V. Grishko and O. Shenderova, *Nanobiotechnology*, 2007, **2**, 37.

- 1 13 X. Kong, L. C. Huang, S. C. Liau, C. C. Han and H. C. Chang, *Anal. Chem.*, 2005, **77**, 4273.
- 14 A. Kruger, Y. Liang, G. Jarre and J. Stegk, *J. Mater. Chem.*, 2006, **16**, 2322.
- 15 A. Krueger, J. Stegk, Y. Liang, L. Lu and G. Jarre, *Langmuir*, 2008, **24**, 4200.
- 5 16 Y. Liu, Z. Gu, J. Margrave and V. Khabashesku, *Chem. Mater.*, 2004, **16**, 3924.
- 17 S. Osswald, G. Yushin, V. Mochalin, S. O. Kucheyev and Y. Gogotsi, *J. Am. Chem. Soc.*, 2006, **128**, 11635.
- 18 N. S. Xu, J. Chen and S. Z. Deng, *Diamond Relat. Mater.*, 2002, **11**, 249.
- 10 19 H. Girard, J. Arnault, S. Perruchas, S. Saada, T. Gacoin, J.-P. Boilot and P. Bergonzo, *Diamond Relat. Mater.*, 2010, **19**, 1117.
- 20 W. S. Yang, O. Auciello, J. E. Butler, W. Cai, J. A. Carlisle, J. Gerbi, D. M. Gruen, T. Knickerbocker, T. L. Lasseter, J. N. Russell, L. M. Smith and R. J. Hamers, *Nat. Mater.*, 2002, **1**, 253.
- 15 21 T. Strother, T. Knickerbocker, J. Russell, J. Butler, L. Smith and R. Hamers, *Langmuir*, 2002, **18**, 968.
- 22 A. Hartl, E. Schmich, J. A. Garrido, J. Hernando, S. C. R. Catharino, S. Walter, P. Feulner, A. Kromka, D. Steinmuller and M. Stutzmann, *Nat. Mater.*, 2004, **3**, 736.
- 23 Y. Zhong and K. Loh, *Chem.-Asian J.*, 2010, **5**, 1532.
- 20 24 M. P. Seah, *Surf. Interface Anal.*, 1989, **14**, 488.
- 25 D. A. Shirley, *Phys. Rev. B: Solid State*, 1972, **5**, 4709.
- 26 J. H. Scofield, *J. Electron Spectrosc. Relat. Phenom.*, 1976, **8**, 129.
- 27 S. Ji, T. Jiang, K. Xu and S. Li, *Appl. Surf. Sci.*, 1998, **133**, 231.
- 28 Y. Liang, M. Ozawa and A. Krueger, *ACS Nano*, 2009, **3**(8), 2288.
- 29 C.-L. Cheng, C.-F. Chen, W.-C. Shiao, D.-S. Tsai and K.-H. Chen, *Diamond Relat. Mater.*, 2005, **14**, 1455.
- 25 30 D. Ballutaud, N. Simon, H. Girard, E. Rzepka and B. Bouchet-Fabre, *Diamond Relat. Mater.*, 2006, **15**, 716.
- 31 L. Ley, R. Graupner, J. B. Cui and J. Ristein, *Carbon*, 1999, **37**, 793.
- 32 S. Ferro, M. Dal Colle and A. De Battisti, *Carbon*, 2005, **43**, 1191.
- 30 33 S. Szunerits and R. Boukherroub, *J. Solid State Electrochem.*, 2008, **12**, 1205.
- 34 M. Wang, N. Simon, G. Charrier, M. Bouttemy, A. Etcheberry, M. S. Li, R. Boukherroub and S. Szunerits, *Electrochem. Commun.*, 2010, **12**, 351.
- 35 J.-S. Tu, E. Perevedentseva, P.-H. Chung and C.-L. Cheng, *J. Chem. Phys.*, 2006, **125**, 174713.
- 36 J. Pinson and F. Podvorica, *Chem. Soc. Rev.*, 2005, **34**, 429.
- 5 37 S. Lud, M. Steenackers, R. Jordan, P. Bruno, D. Gruen, P. Feulner, J. Garrido and M. Stutzmann, *J. Am. Chem. Soc.*, 2006, **128**, 16884.
- 38 L. Tessier, G. Deniau, B. Charleux and S. Palacin, *Chem. Mater.*, 2009, **21**, 4261.
- 39 M. Toupin and D. Belanger, *J. Phys. Chem. C*, 2007, **111**, 3594.
- 10 40 H. Notsu, T. Fukazawa, T. Tatsuma, D. A. Tryk and Y. Fujiwara, *Electrochem. Solid-State Lett.*, 2001, **4**, H1.
- 41 H. Notsu, I. Yagi, T. Tatsuma, D. A. Tryk and A. Fujishima, *Electrochem. Solid-State Lett.*, 1999, **2**, 522.
- 42 T. Ando, K. Yamamoto, M. Ishii, M. Kamo and Y. Sato, *J. Chem. Soc., Faraday Trans.*, 1993, **89**, 3635.
- 15 43 R. Boukherroub, X. Wallart, S. Szunerits, B. Marcus, P. Bouvier and M. Mermoux, *Electrochem. Commun.*, 2005, **7**, 937.
- 44 P. Actis, M. Manesse, C. Nunes-Kirchner, G. Wittstock, Y. Coffinier, R. Boukherroub and S. Szunerits, *Phys. Chem. Chem. Phys.*, 2006, **8**, 4924.
- 45 M. Ozawa, M. Inaguma, M. Takahashi, F. Kataoka, A. Kruger and E. Osawa, *Adv. Mater.*, 2007, **19**, 1201.
- 20 46 O. A. Williams, J. Hees, C. Dieker, W. Jäger, L. Kirste and C. E. Nebel, *ACS Nano*, 2010, **4**, 4824.
- 47 F. Maier, M. Riedel, B. Mantel, J. Ristein and L. Ley, *Phys. Rev. Lett.*, 2000, **85**, 3472.
- 48 C. Bandis and B. B. Pate, *Phys. Rev. Lett.*, 1995, **74**, 777.
- 49 J. B. Cui, J. Ristein and L. Ley, *Phys. Rev. Lett.*, 1998, **81**, 429.
- 25 50 D. Shin, B. Rezek, N. Tokuda, D. Takeuchi, H. Watanabe, T. Nakamura, T. Yamamoto and C. E. Nebel, *Phys. Status Solidi A*, 2006, **203**, 3245.
- 51 F. Maier, J. Ristein and L. Ley, *Phys. Rev. B*, 2001, **64**, 165411.
- 52 C. Mangeney, Z. Qin, S. A. Dahoumane, A. Adenier, F. Herbst, J.-P. Boudou, J. Pinson and M. M. Chehimi, *Diamond Relat. Mater.*, 2008, **17**, 1881.
- 30

35

40

45

50

55